Feasibility of Non-Invasive Determination of the Stability of Propagation Reserve in Patients

SF Idriss[1], W Krassowska Neu[1], V Varadarajan[2], T Antonijevic[2], SS Gilani[2], JM Starobin[2]

[1]Duke University, Durham, NC, USA [2]Joint School of Nanoscience and Nanotechnology, University of North Carolina Greensboro, NC, USA

Abstract

This study investigates the feasibility of using surface ECG recordings to assess stability of cardiac propagation. Our novel method customizes a reaction-diffusion model of cardiac excitation using measurements of patient's repolarization dynamics. The customized model determines the stability-of-propagation reserve (SoPR) that measures the proximity of the patient's minimum level of refractoriness to the critical level associated with conduction instability. Using measurements from 15 patients, we compared SoPRs determined from the unipolar intracardiac electrograms and from the surface ECG leads. SoPRs computed from intracardiac and surface measurements correlated, and a formula was developed that estimated the intracardiac SoPR from surface measurements with 5% accuracy. Thus, this study may lead to new noninvasive tests for the risk of sudden cardiac death.

1. Introduction

Each year approximately 310,000 Americans die of sudden cardiac death from ventricular tachyarrhythmias [1]. Yet, despite years of research, strategies for identifying people at risk still remain unclear [2]. One potential mechanism for arrhythmia has been discovered and involves a change where stable periodic waves of cardiac excitation begin alternating on a beat-to-beat basis. This state, known as alternans, may lead to unidirectional conduction block, reentry, and the onset of a potentially fatal tachyarrhythmia. Some patients at risk for arrhythmias arising through this mechanism can be identified non-invasively with ECG T-wave alternans testing [3].

However, alternans is only one possible route to the development of conduction block and fatal arrhythmias. For example, conduction block may occur if a premature stimulus is applied to the tissue timed when a critical level of refractoriness is present. This may cause conduction block and wavebreak when there is interaction with a less excitable portion of cardiac tissue [4,5]. This mechanism can occur without alternans. Therefore, there is a need for a more general test that could predict vulnerability to conduction block with or without prior alternans.

We have developed a novel method to assess patient's risk for conduction instability. By combining measurements of patient's repolarization dynamics with a reaction-diffusion model of cardiac excitation, we can compute a new metric, the stability-of-propagation reserve (SoPR). SoPR measures the proximity of the patient's minimum level of refractoriness to the critical level associated with conduction instability. In this paper we investigate the feasibility of computing SoPR noninvasively, from surface ECG recordings.

2. Methods

2.1. Patient population, measurements, and signal processing

Clinical measurements were performed after obtaining IRB consent on 15 patients of either genders and different ethnic origins, 13-22 years old. All patients were undergoing electrophysiology (EP) testing and ablation for supraventricular arrhythmias. All had structurally normal hearts with normal ventricular function and without known or suspected ventricular arrhythmias.

A "downsweep" pacing protocol was performed using a clinical EP stimulator. The protocol consisted of six one-minute plateaus of constant-rate pacing with the pacing period *T*, which decreased from 600 to 350 ms in five steps of 50 ms. During the protocol, the surface 12 lead ECG was recorded simultaneously with unipolar electrograms obtained from the right ventricular endocardium using standard quadripolar EP catheters. A clinical EP recording system (GE Prucka) was used for data acquisition. One endocardial lead and surface ECG lead II were used in the analysis.

After completion of each EP study, custom software, written in Labview, was used to remove electrical noise, eliminate pacing stimuli from the signals, and determine the durations of QT and RR intervals.

Over all patients, 81 plateaus of constant pacing were recorded (Fig. 1). At each plateau, steady-state values of QT and RR intervals were determined by averaging the last 25% of data points. The TQ intervals were computed as the difference between RR and QT intervals.

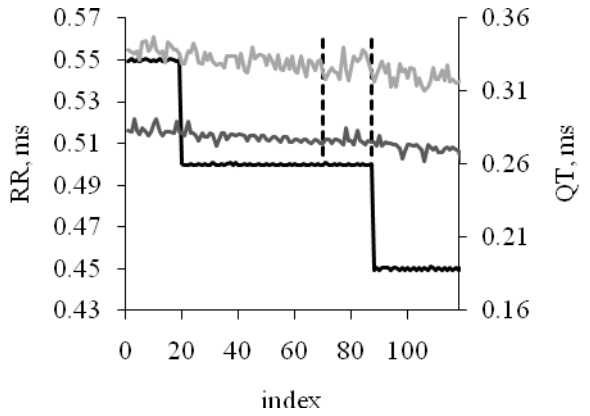

Figure 1. Example sequences of QT and RR intervals showing two downsteps and one full plateau of constant-rate pacing. Black line represents RR intervals; light gray and dark gray lines represent QT intervals from the surface lead II and the RV lead, respectively. Dashed vertical lines show the last 25% of data points in the plateau.

2.2. Reaction-diffusion model and SoPR

Our method uses a two-variable Chernyak-Starobin-Cohen (CSC) reaction-diffusion model, which is analytically solvable and offers a robust criterion for the stability of an excitation wave in a 1D cable [6]. Unlike more detailed ionic models [7,8], the CSC model parameters can be customized based only on measured RR and QT intervals, so it can reproduce the heart rate dynamics of an individual patient. The state variables of the model are the membrane potential *u(x,t)* and recovery variable *v(x,t)*. Both are dimensionless, with values between 0 and 1. The equations governing propagation in a 1D cable with the CSC membrane model are:

$$\frac{\partial u}{\partial t} = \frac{\partial^2 u}{\partial x^2} - i(u,v) + P(x,t) \qquad (2.1)$$

$$\frac{\partial v}{\partial t} = \varepsilon(\zeta u + v_r - v) \qquad (2.2)$$

where membrane current $i(u,v)$ is given by $i(u,v)=\lambda u$ for $u<v$ and $i(u,v)=(u-1)$ for $u \geq v$. $P(x,t)$ specifies the pacing pulses; ε, ζ, λ and v_r are model parameters. At rest, u and v are equal to 0 and v_r, respectively. Figure 2 shows that the potential u quickly increases to 1 during the upstroke, stays near 1 during the action potential (AP), and afterwards returns to zero. The recovery variable v moves slowly toward 1 during the AP and starts decreasing after AP ends.

In order for the model to support propagation of excitation waves, the recovery variable v must drop below a certain value, v_r^{crit} [6]. As illustrated in Fig. 2, during rapid pacing v does not return to its solitary pulse rest value v_r. Instead, it reaches a minimum value v_{min} during the foot of the AP. We have discovered that the proximity of v_{min} to the critical excitation threshold v_r^{crit} of a solitary pulse determines the loss of stability of the propagating waves in a 1D cable [9]. Therefore, we use the normalized difference $(v_{min} - v_r^{crit})$ as a measure of the stability-of-propagation reserve, SoPR:

$$SoPR = \frac{(v_r^{crit} - v_{\min})}{v_r^{crit}} \times 100\% \qquad (2.3)$$

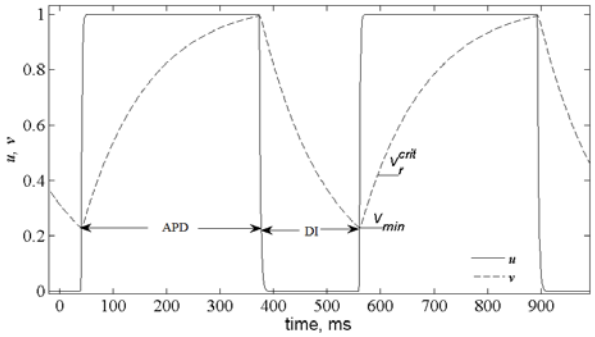

Figure 2. An example of two consecutive responses to pacing stimuli computed from Eqs. (2.1-2.2). Solid and dashed line show time courses of u and v, respectively. Short horizontal lines show values of v_r^{crit} and v_{min}.

2.3. Fitting model parameters

In order to customize the CSC model for individual patients, the model must compute sequences of action potential durations (APD) and diastolic intervals (DI), which can be related to measured QT and TQ intervals. APD and DI were computed using two different methods:

(i) From the *full model:* by solving Eq. (2.1-2.2) numerically in the cable of finite length (20 units) using an explicit difference scheme described in [9].

(ii) From the *singular limit approximation:* for an abrupt change of u from 0 to 1, one can determine analytic expressions for APD and DI by integrating (2.2) at u=0 and u=1, respectively:

$$APD = \frac{1}{\varepsilon}\ln\frac{\zeta + v_r - v_{\min}}{v_r} \qquad (2.4)$$

$$DI = \frac{1}{\varepsilon}\ln\frac{1 - v_r}{v_{\min} - v_r} \qquad (2.5)$$

Next, dimensionless APD and DI values from the model must be converted to dimensional QT^m and TQ^m intervals by:

$$QT^m = \frac{c_m}{\sigma_{Na}} APD;\ TQ^m = \frac{c_m}{\sigma_{Na}} DI \qquad (2.6)$$

where c_m and σ_{Na} are characteristic values of membrane capacitance and sodium membrane conductance. The ratio of c_m and σ_{Na} for normal ventricles is approximately equal to 1 ms [10].

Finally, for each patient the parameters of the CSC model were chosen. The model has four parameters ε, ζ, λ and v_r that need to be determined for each pacing rate. The fitting procedure minimizes the difference Δ_{ss} between the steady state values of the QT^m intervals from the model and the QT intervals measured in the EP study. For the *full model* (2.1-2.2), the minimal value of Δ_{ss} is given by

$$\Delta_{ss} = \min_{\varepsilon,\zeta,\lambda,v_r \in \Omega} \left\{ \sum_{\Omega} \left| \frac{QT^m - QT}{QT^m} \right| + \left| \frac{DI^m - DI}{DI^m} \right| \right\} \times 100\% \qquad (2.7)$$

For the *singular limit approximation*, the fitting procedure includes v_{min} instead of λ because v_{min} appears in Eqs. (2.4-2.5) and λ does not. The initial estimates for all parameters are obtained by searching over a sparse four-dimensional parameter space grid. Parameter estimates are continuously refined using Powell's optimization technique [11]. For each iteration, the new value of QT^m is obtained from the model using the new parameter estimates. Iterations stop when Δ_{SS} decreases below 1%.

3. Results

3.1. Computing intracardiac QT and TQ intervals from surface ECG measurements

The sequences of the QT and TQ intervals from the intracardiac lead (QT_{RV} and TQ_{RV}) were closely related to those from the surface lead II (QT_{II} and TQ_{II}); see Fig. 1 for an example. We found that the median ratio of QT_{RV} to QT_{II} was equal to 0.8606 (Fig. 3). This value is close to cos(30º) and 30º is the mean angular separation between the intracadiac lead RV and the surface lead II. Thus, we can approximate intracardiac values of QT and TQ intervals noninvasively, by using the following formulas:

$$QT_{app} = QT_{II} \times 0.8606 \qquad (3.1)$$

$$TQ_{app} = RR - QT_{app} \qquad (3.2)$$

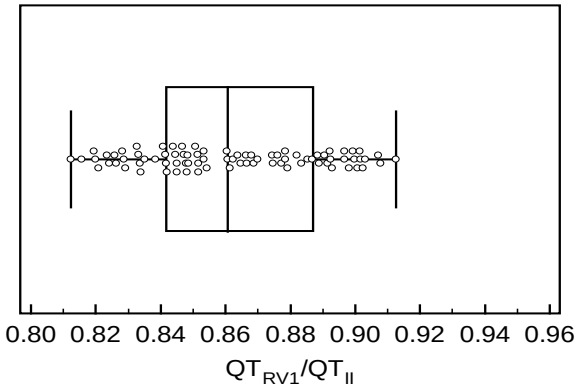

Figure 3. A box plot of the QT_{RV}/QT_{II} ratio of intracardiac and surface QT intervals. The median value 0.8606 is approximately equal to the cos(30º). The 95% confidence interval lies between 0.8491and 0.8697.

3.2. Comparison of SoPR values determined from intracardiac and surface ECG measurements

For each pacing rate in each patient, we determined three estimates of the SoPR:

$SOPR_{RV}$: *Intracardiac* QT and TQ intervals from lead RV were matched to values generated by the *full model* (2.1-2.1).

$SOPR_{app}$: *Surface ECG* QT and TQ intervals from lead II, converted according to (31.-3.2), were matched to values generated by the *full model* (2.1-2.2).

$SOPR'_{app}$: *Surface ECG* QT and TQ intervals from lead II, converted according to (3.1-3.2), were matched to values computed from the *singular limit* equations (2.4-2.5).

Figure 4 compares these three estimates of the SoPR. We found that the group-wise separation of SoPR values between different estimates was statistically insignificant. Specifically, non-invasive and invasive estimates, $SOPR_{RV}$ and $SOPR_{app}$, were practically the same (t-test for independent samples, p>0.5). Likewise,

estimates obtained by fitting the full model, $SOPR_{app}$, were close to those determined from fitting the singular limit solution, $SOPR'_{app}$ ($p>0.1$). In both cases, the corresponding relative errors between values of $SOPR_{app}$, $SOPR'_{app}$, and $SOPR_{RV}$ were smaller than 5%.

Note that in Fig. 4, $SOPR_{RV}$ and $SOPR_{app}$ values appear only for 61 pacing plateaus with DI>120 ms. This is because for shorter DIs fitting QT and TQ intervals to the full model (2.1-2.2) resulted in a high optimization error exceeding 1%. In contrast, using the singular limit equations (2.4-2.5) provided satisfactory SoPR estimates for all diastolic intervals, including those shorter than 120 ms. Moreover, singular limit-based fitting was generally more accurate, with $\Delta_{ss} << 1\%$.

Figure 4 also shows that the SoPR depends on DI. As expected, values of SoPR decrease as the pacing rate becomes faster, indicating the approach to the boundary of conduction stability.

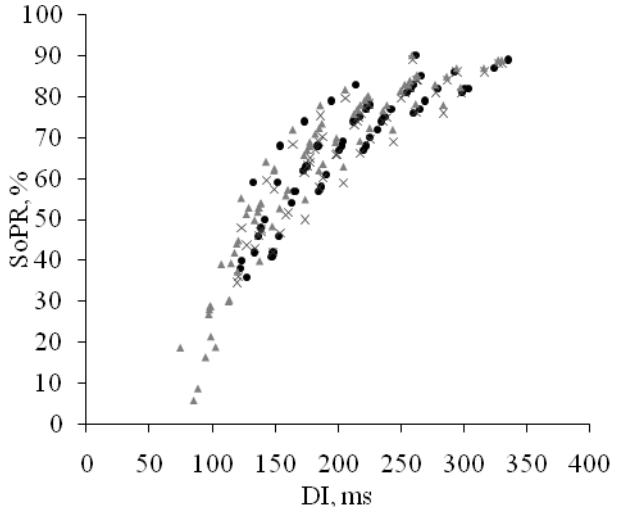

Figure 5. Dependence of SoPR on the diastolic interval DI for all patients and all pacing plateaus. Black dots (•) represent the invasively-measured $SOPR_{RV}$, symbols (x) represent the noninvasive approximation $SOPR_{app}$, and triangles (▲) represent $SOPR'_{app}$ computed using the singular limit equations.

4. Conclusions

In this study, we tested a noninvasive approach to estimating the stability-of-propagation reserve in patients with normal ventricular function. We found that SoPRs determined from invasive intracardiac measurements are practically the same as SoPRs approximated using surface ECG measurements that were recalculated based on a thirty degree lead projection determined by the Einthoven triangle. We also found that using the singular limit equations while fitting the model to patient's EP measurements is more accurate than using the full model and it works for diastolic intervals shorter than 120ms, where the full model-based fitting fails.

All estimates of the SoPR computed in this study were positive, which is expected for healthy hearts and agrees with the clinical observation that conduction block was not detected in any patients at any pacing rate. The decrease of SoPR values with increasing pacing rate is consistent with the substrate approaching to the border of conduction instabilities. Therefore, these preliminary results warrant further investigation of the ability of SoPR to predict conduction blocks in populations with different ventricular dysfunctions.

Acknowledgements

This research was supported by the American Heart Association grant 10CPR3040018.

References

[1] Lloyd-Jones D, Adams R, Carnethon M, et al. Heart disease and stroke statistics 2009 update, Circulation, 2009:119: e1-e161.

[2] Kusmirek SL, Gold MR. Sudden cardiac death: The role of risk stratification. Am. Heart J. 2997;153:S25-S33.

[3] Walker ML, Rosenbaum DS. Repolarization alternans: implications for the mechanism and prevention of sudden cardiac death, Cardiovasc. Res 2003;57: 599-614.

[4] Starobin J, Zilberter YI, Starmer CF. Vulnerability in one-dimensional excitable media, Physica D 1994;70: 321-341.

[5] Starobin JM, Zilberter YI, Rusnak EM, et. al. Wavelet formation in excitable cardiac tissue: The role of wavefront-obstacle interaction in initiating high-frequency fibrillatory-like arrhythmias, Biophys. J 1996;70: 581-594.

[6] Chernyak YB, Starobin JM, Cohen RJ. Class of exactly solvable models of excitable media, Phys. Rev. Lett 1998;80:5675-5678.

[7] Beeler GW, Reuter H. Reconstruction of the action potential of ventricular myocardial fibres. J. Physiol 1977;268:177-210.

[8] Luo C, Rudy Y. A dynamic model of the cardiac ventricular action potential, Circ. Res. 1994;74:1071-1096.

[9] Starobin JM, Danford CP, Varadarajan V, et. al. Critical scale of propagation influences dynamics of waves in a model of excitable medium, Nonlinear Biomedical Physics 2009;3: art. 4.

[10] Plonsey R., Barr R. C. Bioelectricity: a quantitative approach. Kluwer Academic/Plenum Publishers, New York, 2000.

[11] Press WH, Teukolsky SA, Vetterling WT, Flannery BP. Numerical recipies in Fortran 77: The art of scientific computing. Cambridge University Press, New York, 2001.

Address for correspondence.

Starobin J.M.
JSNN, 2907 E.Lee St., Room 208F, Greensboro, NC 27401
jmstarob@uncg.edu